
Contents

1 Scheduling in cognitive networks	
<i>Chandrasekharan Raman, Jasvinder Singh, Roy D. Yates,</i>	
<i>Narayan B. Mandayam</i>	1
1.1 Introduction	1
1.2 System Model	4
1.3 Maximum sum rate scheduling	7
1.4 Fair Scheduling	8
1.4.1 Max-min fairness	9
1.4.2 Proportional fairness	10
1.5 Distributed Dynamic Spectrum Access Policies	10
1.5.1 Rate Regions	12
1.5.2 Characterization of rate region for the decentralized scheme ...	13
1.5.3 Distributed Algorithm	14
1.6 Cross layer scheduling of end-to-end flows	16
1.7 Simulation Results	18
1.8 Conclusion	20
References	21
Index	25

List of Contributors

Chandrasekharan Raman
WINLAB, Rutgers
671 US Route 1 South
North Brunswick, NJ 08902.
chandru@winlab.rutgers.edu

Jasvinder Singh
WINLAB, Rutgers
671 US Route 1 South
North Brunswick, NJ 08902.
jasingh@winlab.rutgers.edu

Roy D. Yates
WINLAB, Rutgers
671 US Route 1 South
North Brunswick, NJ 08902.
ryates@winlab.rutgers.edu

Narayan B. Mandayam
WINLAB, Rutgers
671 US Route 1 South
North Brunswick, NJ 08902.
narayan@winlab.rutgers.edu

Scheduling in cognitive networks

Scheduling variable rate links – centralized and decentralized approaches

Chandrasekharan Raman, Jasvinder Singh, Roy D. Yates and Narayan B. Mandayam

WINLAB, Rutgers - The State University of NJ.

Summary. In this chapter, we present an optimization framework for link level and flow level scheduling in cognitive radio networks. In the centralized scheduling framework, a spectrum server coordinates the transmissions of a group of links sharing a common spectrum. With knowledge of the link gains in the network, the spectrum server schedules the on/off periods of the links so as to satisfy constraints on link fairness. We then compare the throughput regions of centralized scheduling and a probabilistic random access scheme, wherein in each slot, a link is active with a fixed probability chosen independent of other interfering links. We observe that for the case of two interfering links, the probabilistic scheme does not suffer any loss in the rate region relative to the centralized scheme if the interference between the links is sufficiently low. We then present a distributed algorithm where each link independently updates its transmission probability based on its measured throughput to achieve any desired feasible rate vector in the throughput region of the probabilistic scheme and prove its convergence. Finally, we present an optimization framework for end-to-end flow level scheduling of flows in network with mutually interfering links.

1.1 Introduction

The emergence of unlicensed spectrum has spawned an impressive variety of important technologies and innovative uses, ranging from scientific and industrial to domestic applications and systems. Since these systems must adapt to a wide variety of unpredictable conditions, the emerging technologies called “cognitive radio” [17] offer significant potential benefits in system capacity and service quality.

In their simplest embodiments (which are by no means simple to implement) cognitive radios can recognize the available systems and adjust their frequencies, waveforms and protocols to access those systems efficiently [16]. Not surprisingly, it is upon these difficult “design” issues that most current research activities are focused, as illustrated by some chapters in this book. For instance, some physical layer design issues related to cognitive radios are

discussed in [5] while some issues related to sensing are addressed in [34, 35]. While these basic capabilities represent a difficult and significant step forward, they fail to fully illuminate the effects of cognitive behavior. When there exist methods by which cognitive radios can independently discover local information, a variety of physical layer, system and network layer protocols can be applied to allow cooperation and coexistence. However, such levels of cooperation and interoperability may not be possible when multiple services and systems must coexist. In a heterogeneous environment, some users may look to obtain high data rates without regard to energy efficiency; other users may wish to transmit at a fixed rate but with high efficiency. In certain applications, it will be important to enforce fairness constraints. In general, the system performance will have a multidimensional characterization. These dimensions often represent conflicting performance measures. In this chapter, we take a step towards characterizing some of these performance measures.

In the realm of cognitive radio networks, two distinct sets of issues emerge. First, for a given set of transmitter and receiver technologies and a specified set of performance constraints, one must resolve the multidimensional boundaries of system performance. As we shall see, this is a difficult problem, even if complete system state information is available to all network nodes. Second, the collection of intelligent adaptation policies of the individual nodes constitute a large distributed system for spectrum allocation. A given set of distributed information gathering and exchange mechanisms may greatly influence the performance of the system.

This work tries to separate these issues. We examine the boundaries of system performance under the assumption that efficient open access to spectrum can be resolved by an impartial “spectrum server” [4] that can obtain information about the interference environment through measurements contributed by different terminals, and then offer suggestions for efficient coordination to interested service subscribers. In this work, the spectrum server is a centralized scheduler that uses full knowledge of the network configuration to specify the activity patterns of the individual links. Our aim is to provide upper-bounds on the performance of distributed adaptive scheduling methods based on the performance of the spectrum server. We then characterize the loss in performance of a simple distributed random access scheme.

It is recognized that the nodes of a cognitive radio network can interact in a variety of (arbitrary) ways. To distill these interactions, we see that each radio follows a transmission policy (specified here for instance by the spectrum server) that results in signals that vary over time, frequency, and space. This variation may be the result of adaptation to measurements of channels or interference. The performance of a particular signaling strategy depends on each receiver’s ability to resolve signals in the presence of interfering transmissions. In this work, we do not assume any specific physical layer transmission technique, but abstract out the essential features of any technique into a rate matrix.

For a system of interfering wireless transmissions, a mathematical model starts with a basis for signal space. Each user employs a combination of basis functions to transmit in some or all of the signal dimensions. This work assumes a relatively simple signaling structure: signals are time-slotted transmissions over a frequency-flat channel. The interference that a receiver faces depends on the subset of nodes transmitting in that time slot. The structure of the transmitted signals (spread or unspread, coded or not) and the receiver technology determines the ability of the node to separate a desired signal from the interference. Thus, the data rate that a link can obtain in a time slot depends on the subset of nodes that are actively transmitting in that slot.

There are many ways in which a spectrum server can coordinate a network of cognitive radios. The work in [18] considers the spectrum server's role in demand responsive pricing and competitive spectrum allocation. In [27], the spectrum server aids the users' decision in forming stable coalitions among themselves so as to maximize the sum throughput in the network. In this work, the spectrum server specifies the schedule of transmission for mutually interfering users sharing a common spectrum.

Scheduling transmissions in a wireless network has been studied in various contexts outside of cognitive radio. Though link scheduling is a difficult problem to solve [15], joint optimization of scheduling and routing in a cross-layer framework has been studied by lot of researchers in recent years. In [9], a joint scheduling and power control strategy is proposed to maximize network throughput and energy efficiency of the system. Another direction in this problem is addressed in [8], where the authors look at the cross-layer issues of routing, scheduling and power control. Other related works include [19,23,40].

In the centralized scheduling framework, we assume that we obtain a non-zero rate in the links for any non-zero signal-to-interference ratio (SIR). If the link gains are known to the spectrum server, it can schedule the transmissions among the links to maximize the system throughput. The optimization problem, subject to minimum rate constraints in the individual links, is posed as a linear program. It is shown that when there is no minimum rate constraint, a fixed set of links (called the dominant mode) that maximizes the sum rate is operated all the time. In order to offset the inherent unfairness in the above solution, we introduce a minimum rate constraint in each link. We observe that the max-min fair rate allocation can be obtained in one step by solving a linear program which maximizes the minimum common rate among the links. The optimization framework for proportional fair scheduling is posed as a non-linear program.

In the distributed scheduling framework, we compare the throughput regions of centralized scheduling and a probabilistic random access scheme, wherein in each slot, a link is active with a fixed probability chosen independent of other interfering links. We observe that for the case of two interfering links, the probabilistic scheme does not suffer any loss in the rate region relative to the centralized scheme if the interference between the links is sufficiently low. For more than two interfering links, the characterization

of throughput rate region for the probabilistic scheme becomes intractable and similar observations are not easily forthcoming. However, we give a distributed algorithm where each link independently updates its transmission probability based on its measured throughput to achieve any desired feasible rate vector in the throughput region of the probabilistic scheme and prove its convergence.

Finally, we present the cross-layer optimization framework for end-to-end flow scheduling for a network supporting variable rates because of mutual interference.

1.2 System Model

Before we explain the system model, we comment on the notation of this chapter. We use boldface lowercase characters for vectors and boldface uppercase for matrices. If \mathbf{a} is a vector, \mathbf{a}^T denotes its transpose and $\mathbf{a}^T \mathbf{b} = \sum_i a_i b_i$ represents the inner product of the vectors \mathbf{a} and \mathbf{b} . The vector of all zeros and all ones are represented by $\mathbf{0}$ and $\mathbf{1}$ respectively. Inequalities between vectors are component-wise inequalities.

We consider a wireless network with N nodes forming L logical links sharing a common spectrum. The network can be represented as a directed graph $\mathcal{G}(\mathcal{V}, \mathcal{E})$, where the nodes in the network are represented by the set of vertices \mathcal{V} of the graph and the links are represented by a set of directed edges \mathcal{E} . Therefore the cardinalities $|\mathcal{V}| = N$ and $|\mathcal{E}| = L$. A directed edge from a node m to node n implies that m wishes to communicate data to node n . We consider the scenario where the spectrum server coordinates the activity of the set of L links to share the spectrum efficiently.

Define the set of *transmission modes* $\mathcal{T} = \{0, 1, \dots, M-1\}$, where $M = 2^L$ denotes the number of possible transmission modes. Then the *mode activity vector* \mathbf{t}_i of mode i is a binary vector, indicating the on-off activity of the links. If $\mathbf{t}_i = [t_{1i}, t_{2i}, \dots, t_{Li}]^T$ is a mode activity vector, then

$$t_{li} = \begin{cases} 1, & \text{if link } l \text{ is active under transmission mode } i, \\ 0, & \text{otherwise.} \end{cases} \quad (1.1)$$

Note that there are M possible transmission modes including the mode with activity $[0, 0, \dots, 0]^T$ in which all links are off. Figure 1.1 shows a representative network and Figure 1.2 shows a particular transmission mode for the set of links.

Let the transmitter power on a link $l \in \mathcal{E}$ be P_l . If G_{lk} is the link gain from the transmitter of link k to the receiver of link l and σ_l^2 is the noise power at the receiver of link l , the Signal-to-Interference Ratio (SIR) γ_{li} at the receiver of link l in transmission mode i is given by

$$\gamma_{li} = \frac{t_{li} G_{ll} P_l}{\sum_{k \in \mathcal{E}, k \neq l} t_{ki} G_{lk} P_k + \sigma_l^2}. \quad (1.2)$$

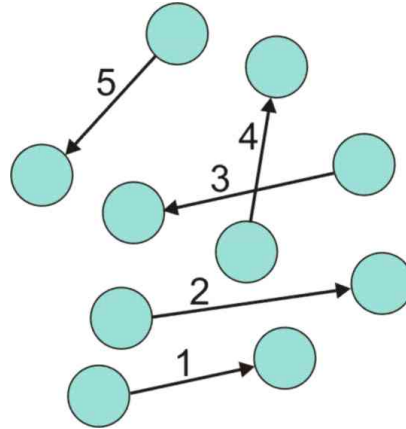


Fig. 1.1. Graph of network showing the nodes and directed links

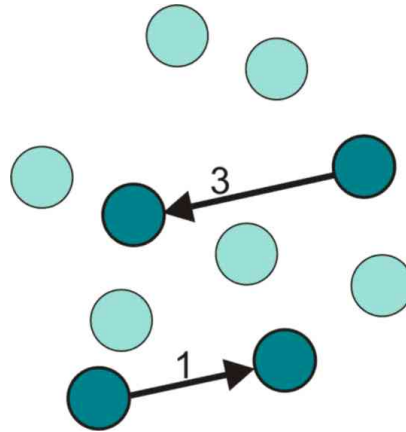


Fig. 1.2. Graph of network showing transmission mode corresponding to (1 0 1 0)

It is assumed that the link gain between a transmitter and receiver takes into account the path loss and attenuation due to shadow fading. The data rate in each link depends on the SIR in that link. We assume that the transmitter can vary its data rate, possibly through a combination of adaptive modulation and coding. In particular, for a given mode, the transmitter and receiver on a link employ the highest rate that permits reliable communication given the link SIR in that mode. For purposes of this study, we assume that the transmission of other links are treated as Gaussian noise and that a transmission on link l is reliable in a given mode i with a data rate

$$c_{li} = \log(1 + \gamma_{li}). \tag{1.3}$$

This same interference model is also employed in [6, 11]. We emphasize here that we do not consider any minimum SIR threshold required at the receiver. A non-zero γ_{li} in each transmission mode i defines a non-zero rate on the link l . Let x_i be the fraction of time that transmission mode i is active and r_l be the average data rate of link l . The average data rate in link l is the time average of the data rates of all the transmission modes that include link l . Thus,

$$r_l = \sum_i c_{li}x_i, \quad (1.4)$$

or in vector form,

$$\mathbf{r} = \mathbf{C}\mathbf{x}, \quad (1.5)$$

where $\mathbf{C} = [\mathbf{c}_1 \ \mathbf{c}_2 \ \dots \ \mathbf{c}_M]$ is an $L \times M$ matrix with non-negative entries, such that its j th column $\mathbf{c}_j = [c_{1j}, c_{2j}, \dots, c_{Lj}]^T$ contains the rate obtained by each link in mode j . The idea of transmission modes to model a set of transmitter-receiver pairs has been used in [7, 43] previously. In this work, we use such a model as basis specify schedules that maximize the system throughput, subject to minimum rate and fairness constraints.

In practice, a scheduler will specify a sequence of transmission modes. Typically, this would be done by constructing a frame with N time slots and allocating N_j time slots to each mode j . The fraction of time that mode j is active will be $x_j = N_j/N$. For sufficiently large N , the ratio N_j/N can be made arbitrarily close to any $x_j \in [0, 1]$. In this case, the average rate \mathbf{r} in (1.5) will represent the average link data rates over one frame. For our analytical model, we optimize these average rates per frame by specification of the time fractions in \mathbf{x} , without explicitly specifying the precise slots assigned to each mode. We denote the set of all feasible schedule vectors by

$$\mathcal{X} = \{\mathbf{x} : \mathbf{1}^T \mathbf{x} = 1, \mathbf{x} \geq \mathbf{0}\}. \quad (1.6)$$

We note that this model has a number of desirable characteristics. First, we observe that all aspects of transmitter and receiver technology are embedded in the rate matrix \mathbf{C} . For example, if the links employed CDMA spreading, Equation (1.2) for the SIR on link l in mode j would be appropriately modified, as in [44] for example, to reflect the transmitter spreading sequences and receiver filter vectors used in that mode. Similarly, if we were to assume a particular practical coding and modulation scheme, we would modify Equation (1.3) for the expected number of bits that we would expect to decode at a specified SIR. If the nodes employ multiaccess techniques like interference cancellation or multiuser detection, the rates in the \mathbf{C} matrix are calculated according to the multiaccess rates that can be achieved in each transmission mode. Thus the general model allows for consideration of a large class of physical layer interactions. We employ the specific choices in Equations (1.2) and (1.3) to demonstrate tradeoffs in between average rates and various fairness constraints.

In addition, consider the average link rates obtained by an arbitrary dynamic spectrum access system. Each link employs a dynamic policy, based on measurements and perhaps some side information, to determine when to be active. At any given time, some subset of links will be active and the rates obtained on each link will be determined by the interference generated by those active links. In short, any dynamic spectrum access system yields a series of transmission modes. The rate obtained by each link l in each mode j will be given by c_{lj} . To speak of average rates for the links, the collection of link access policies must yield an ergodic transmission mode process such that we can define x_j as the fraction of time the system is in mode j . In this case, the average link data rates will be given by (1.5). In short, any set of average rates obtained by a dynamic spectrum access system can also be obtained by a centralized scheduler that specifies the identical time fraction x_j for each mode j . Thus the centralized scheduler allows us to separate what average link rates can be obtained from the issue of whether a dynamic system can achieve those rates.

1.3 Maximum sum rate scheduling

A centralized scheduling approach is better suited to optimize the overall utility of the network as it can have access to global information about the nodes of the network. A wide variety of objective functions have been proposed in the literature depending on the driving application, e.g., [13]. In this work, as a first step, we are interested in finding the schedule that maximizes the sum of the average data rates over all links $l = 1, 2, \dots, L$, subject to constraints on the minimum rates for each link. The optimization problem for finding the maximum sum rate schedule can be posed as the following linear program (LP):

$$\max \quad \mathbf{1}^T \mathbf{r} \quad (1.7)$$

$$\text{subject to} \quad \mathbf{r} = \mathbf{C}\mathbf{x}, \quad (1.7a)$$

$$\mathbf{r} \geq \mathbf{r}_{\min}, \quad (1.7b)$$

$$\mathbf{x} \in \mathcal{X}. \quad (1.7c)$$

where, the objective function $\mathbf{1}^T \mathbf{r} = \sum_i r_i$ is the sum of average rates of the individual links and the constraint (1.7b) represents the minimum rate requirement of the links.

The variables in the LP (1.7) are \mathbf{r} and \mathbf{x} . Rewriting the LP in terms of a single variable \mathbf{x} , we have

$$c_{opt}(\mathbf{r}_{\min}) = \max \quad \mathbf{1}^T \mathbf{C}\mathbf{x} \quad (1.8)$$

$$\text{subject to} \quad \mathbf{C}\mathbf{x} \geq \mathbf{r}_{\min}, \quad (1.8a)$$

$$\mathbf{x} \in \mathcal{X}. \quad (1.8b)$$

In the special case when minimum rate constraint $\mathbf{r}_{\min} = \mathbf{0}$, the transmission mode corresponding to the highest sum rate is always operated. The maximum sum rate $c_{opt}(\mathbf{0})$ is equal to the maximum column sum of the rate matrix \mathbf{C} [33]. This is true because

$$\mathbf{1}^T \mathbf{C} \mathbf{x} = \sum_{l=1}^L \sum_{i=1}^M c_{li} x_i = \sum_{i=1}^M x_i \sum_{l=1}^L c_{li} \leq \max_i \sum_{l=1}^L c_{li}, \quad (1.9)$$

where the inequality in (1.9) is true since $\sum_i x_i = 1$. Equality holds in (1.9) when $\mathbf{x} = \mathbf{x}_{opt} = [0 \ 0 \dots 1 \dots 0 \ 0]^T$ where the position of 1 in \mathbf{x}_{opt} is $\hat{i} = \arg \max_i \sum_{l=1}^L c_{li}$. We refer to \hat{i} as the *dominant transmission mode*. The dominant mode could consist of a single link or a collection of links depending on the topology of the network. However, the links that are not a part of the dominant mode are not operated at all. Since we are maximizing a global objective function like sum rate of the network, there is an inherent unfairness in the system.

In order to offset the unfairness in the system, we introduce a non-zero minimum rate requirement in the individual links of the network. In such cases, the optimal schedule balances the use of the dominant mode against modes that provide non-zero rates to the otherwise disadvantaged links. This, however, comes at the cost of reduction in the sum rate of the network. The loss in sum rate due to the minimum rate constraint was characterized in [33].

There exists a trade-off between the sum rate and individual rates of the links, i.e., when we increase the minimum rate requirement in the links, the sum rate obtained decreases. This is intuitively satisfying since the dominant mode, which offers the highest sum rate, is always turned on whenever there is no minimum rate requirement on the links. When the minimum rate requirement is increased from zero, other transmission modes are forced to be scheduled for transmission in order to satisfy the minimum rate requirement of the links. Since the modes other than the dominant mode always offer a lesser sum rate than the dominant mode, the sum rate decreases monotonically with increase in required minimum rate. The minimum rate requirement for all links in the network can be increased by trading off sum rate until it is infeasible to support the rate requirement in all links.

1.4 Fair Scheduling

In the previous section, we observed that maximizing the sum rate without minimum rate constraints leads to unfairness among the links. More fundamentally, the underlying shared wireless medium and the global objective function bring up the question of fairness. We investigate fair scheduling strategies in this section. We start with the conventional max-min fair objective.

1.4.1 Max-min fairness

Definition 1 A vector of rates \mathbf{r} is said to be max-min fair if it is feasible and for each $l \in \mathcal{E}$, r_l cannot be increased while maintaining feasibility without decreasing $r_{l'}$ for some link l' for which $r_{l'} \leq r_l$. Formally, for any other feasible allocation $\tilde{\mathbf{r}}$, with $\tilde{r}_l > r_l$, there must exist some l' such that $\tilde{r}_{l'} < r_{l'} \leq r_l$.

Max-min fairness is well studied in the context of flow control of elastic traffic in data networks [1]. Fairness in wireless networks have been studied in [20,28,41]. Our model differs from the data networks model, wherein there could be many sessions flowing through multiple links of finite capacity. There may be several bottleneck links and a feasible rate allocation is max-min fair if and only if all flows pass through at least one bottleneck link [1]. However, in our model, each link has a minimum rate requirement to satisfy and it is not clear as to what constitute the system bottlenecks. Even if we could answer this question, the next important question is: how many bottlenecks are there in the system? Given that the max-min fair set of rates exist, how do we compute them? We try to answer these questions in this section.

In order to obtain the max-min fair schedule in our setting, we begin by formulating the LP that maximizes the minimum common rate in all the links. The LP is given by

$$r^* = \max \quad r_{\min} \quad (1.10)$$

$$\text{subject to} \quad \mathbf{r} = \mathbf{C}\mathbf{x}, \quad (1.10a)$$

$$\mathbf{r} \geq r_{\min}\mathbf{1}, \quad (1.10b)$$

$$\mathbf{x} \in \mathcal{X}. \quad (1.10c)$$

We now have the following theorem.

Theorem 1. *If the link gains G_{lj} are all non-zero, then any solution to the LP (1.10) results in the unique rate vector $\mathbf{r}^* = r^*\mathbf{1}$.*

The proof of Theorem 1 appears in [33]. In the context of multi-hop flows in wireless networks, a similar result, called the *solidarity property*, was derived by Radunovic et. al in [32]. Since the LP (1.10) which maximizes the common rate among the links, achieves equal rates for all links, the following corollary follows from the definition of max-min fairness.

Corollary 1. *The solution \mathbf{x}^* obtained by solving the LP (1.10) results in the max-min fair rate allocation.*

Note that the corollary reveals that the max-min fair rates can be obtained in one step by solving the LP (1.10), in contrast to the usual iterative computation of max-min fair rates of multiple flows through finite capacity links in wired networks [1] and multihop flows in wireless networks [41]. This difference is due to the fact that there is a single bottleneck – the shared wireless

bandwidth – in the network. As a result, so long as any link perceives non-zero interference from all other links in the network, the maximum common rate among the links is the max-min fair rate.

1.4.2 Proportional fairness

Proportional fairness is another fairness criteria which is popular in the context of scheduling of wireless links. It has been studied in the context of multiuser diversity [42] and downlink scheduling for HDR [37].

Definition 2 *A feasible vector of rates \mathbf{r} is proportional fair if for any other feasible vector \mathbf{r}' , the aggregate of proportional change is negative:*

$$\sum_i \frac{r'_i - r_i}{r_i} \leq 0. \quad (1.11)$$

In [21], Kelly proposed proportional fairness in the context of rate control for elastic traffic. It was also shown that the proportionally fair vector is the one that maximizes the sum of logarithms of the utility functions. We follow a similar approach to obtain the proportional fair rates, we solve the following non-linear optimization problem with linear constraints:

$$\max \quad \sum_l \log r_l \quad (1.12)$$

$$\text{subject to} \quad \mathbf{r} = \mathbf{C}\mathbf{x}, \quad (1.12a)$$

$$\mathbf{x} \in \mathcal{X}. \quad (1.12b)$$

The objective function of the above non-linear optimization problem is increasing and strictly concave. The constraint set is linear and hence the problem is a convex optimization problem [3]. This implies that the problem has a unique global maximum over the constraint set. The solution for such problems can be found out by gradient search algorithms.

Energy conservation in wireless systems is essential to enhance the lifetime of each individual node and the overall life of the network [12]. In certain applications, it may be required that the schedule conforms to stringent energy constraints in the network [10]. Efficient scheduling with constraints on the energy in each node of the network is studied in [46].

1.5 Distributed Dynamic Spectrum Access Policies

The centralized scheduling strategies that have been presented thus far, require information about all the links to be available at the spectrum server. There are many reasons why such a centralized scheduler may be difficult to implement in a real world situation, including:

1. Complete information about all the links and their channel gains should be known to the spectrum server to solve the scheduling problem precisely.
2. If the number of the links increases, the size of the LP increases exponentially.
3. The exchange of information between the centralized spectrum server and the individual transmitters may not be an easy task.

An alternative to approaching the spectrum management problem in a centralized way is to adopt device-centric spectrum management schemes [48]. A device-centric scheme corresponds to each user taking independent actions based on local interference measurements. Such actions might include channel switching [29,30], deciding whether to transmit or not during a time slot [47], changing transmission power levels, or modulation waveforms [6,39]. Under the general framework of transmission modes introduced earlier, such schemes will result in a time sequence of network transmission modes. If the devices use ergodic spectrum access policies, then their aggregate behavior will induce a probability distribution on the network transmission modes, and the average rates achieved by the devices under those set of policies can then be defined over the induced probability distribution. Since lack of coordination between the devices can only reduce the set of achievable rates by the devices, a centralized spectrum management scheme for a given network model will act as a benchmark for a decentralized or device-centric scheme. Device-centric random access schemes, e.g., ALOHA have been widely used in practical multiple access systems. The CSMA/CA schemes used in the IEEE 802.11 networks are very popular, thanks to the ease of implementation and decentralized control of these random access techniques. Of late, research effort has been directed towards analyzing the performance of these random access schemes. In [20,45], the authors propose distributed approaches for fair random access. The throughput characteristics of random access schemes have been studied in [22,26]. A recent work [14] characterizes the Pareto boundary of the network throughput region as the family of solutions optimizing a weighted proportional fairness objective, parametrized by weights chosen by the links. The authors also propose a distributed random access scheme to achieve a desired point within the Pareto optimal boundary.

In this section we present a simple device-centric spectrum access policy for the system model from the previous section (i.e. links use constant power and turn on and off in each time slot). Instead of following a transmission schedule computed and prescribed by a centralized entity, each link is active with a fixed probability chosen independently of the other links in each slot. A given set of transmission probabilities chosen by the users results into a unique average rate vector achieved at the links. We first compare the achievable rate region for this device-centric spectrum access scheme with that of the centralized case, and then provide a distributed algorithm to compute the transmission probabilities corresponding to a vector of average rates desired at the links.

1.5.1 Rate Regions

We define the *rate region* as the set of rate vectors that can be achieved by a dynamic spectrum access scheme. The rate regions for the centralized scheduling scheme and the device-centric spectrum access scheme are discussed below.

Centralized scheme

In this scheme, a schedule is specified by the fractions of time each transmission mode is active. As discussed in the previous section, the spectrum server can be used to compute the the optimum time fractions of activity, to maximize a certain utility function. Let x_j be the fraction of time transmission mode j is active and r_l be the average data rate of link l . The average data rate in link l is the time average of the data rates of all the transmission modes that include link l . Thus,

$$r_l = \sum_j c_{lj}x_j, \quad (1.13)$$

and in vector form,

$$\mathbf{r} = \mathbf{C}_L \mathbf{x}. \quad (1.14)$$

The rate region for the centralized scheduling scheme is given by

$$\mathcal{R}_L^S := \{(r_1, \dots, r_L) : \mathbf{r} = \mathbf{C}_L \mathbf{x}, \mathbf{x} \in \mathcal{X}\}. \quad (1.15)$$

Clearly, the region \mathcal{R}_L^S is a polytope defined by its 2^L vertices which are given by the column vectors of \mathbf{C}_L .

Device-centric Spectrum Access Scheme

In this scheme, link l transmits with a probability p_l chosen independent of the other links in the network. The rate region for the random access scheme is given by

$$\mathcal{R}_L^P := \{(r_1, \dots, r_L) : \mathbf{r} = \mathbf{C}_L \mathbf{x}, \mathbf{x} = \mathbf{f}(\mathbf{p}), \mathbf{0} \leq \mathbf{p} \leq \mathbf{1}\} \quad (1.16)$$

where $\mathbf{f} : \mathbb{R}^L \rightarrow \mathbb{R}^{2^L}$ is given by

$$\mathbf{f}(\mathbf{p}) = \begin{bmatrix} (1-p_1)(1-p_2)\dots(1-p_L) \\ p_1(1-p_2)\dots(1-p_L) \\ \vdots \\ (1-p_1)p_2\dots p_L \\ p_1\dots p_L \end{bmatrix}. \quad (1.17)$$

It is easy to see that $\mathcal{R}_L^P \subseteq \mathcal{R}_L^S$. Also, since $\mathbf{f}(\cdot)$ is a continuous mapping, the set $\{\mathbf{x} : \mathbf{x} = \mathbf{f}(\mathbf{p}), 0 \leq \mathbf{p} \leq \mathbf{1}\}$ must be a closed and continuous region and therefore \mathcal{R}_L^P must also be closed and continuous. Our aim will be to characterize the Pareto boundary of \mathcal{R}_L^P and identifying the conditions, if any, under which $\mathcal{R}_L^P \equiv \mathcal{R}_L^S$. We consider the simple case $L = 2$ to obtain insight into the shape of the rate regions.

1.5.2 Characterization of rate region for the decentralized scheme

Let α and β be the normalized rates achieved the links when both the links are simultaneously active.¹ Then the rates on two links are

$$r_1 = p_1(1 - p_2) + \alpha p_1 p_2, \tag{1.18}$$

$$r_2 = (1 - p_1)p_2 + \beta p_1 p_2. \tag{1.19}$$

The above equations can be rewritten as

$$r_1 = p_2(p_1\alpha + (1 - p_1).0) + (1 - p_2)(p_1.1 + (1 - p_1).0), \tag{1.20}$$

$$r_2 = p_2(p_1\beta + (1 - p_1).1) + (1 - p_2)(p_1.0 + (1 - p_1).0). \tag{1.21}$$

In vector form,

$$\begin{aligned} \begin{bmatrix} r_1 \\ r_2 \end{bmatrix} &= p_2 \left(p_1 \begin{bmatrix} \alpha \\ \beta \end{bmatrix} + (1 - p_1) \begin{bmatrix} 0 \\ 1 \end{bmatrix} \right) \\ &+ (1 - p_2) \left(p_1 \begin{bmatrix} 1 \\ 0 \end{bmatrix} + (1 - p_1) \begin{bmatrix} 0 \\ 0 \end{bmatrix} \right) \end{aligned} \tag{1.22}$$

The above representation of the rate vector, as a nested convex combination of the polytope vertices, is useful in visualizing the rate region \mathcal{R}_2^P . We now consider two different cases.

Low Interference Case : $\alpha + \beta \geq 1$

Figure 1.3 shows \mathcal{R}_2^S . Any point in the quadrilateral $OABC$ can be achieved using centralized scheduling. Notice that the vertices of the polytope $OABC$ are the columns of \mathbf{C}_2 . For a given probability vector $\mathbf{p} = [p_1 \ p_2]^T$, the rate vector \mathbf{r} given by (1.22) is shown as point F in Figure 1.3. As p_1 varies between 0 and 1, points D and E completely trace the line segments AB and OC respectively. As p_2 varies between 0 and 1, the point F traverses the line segment ED completely. Hence, it can be seen that by varying \mathbf{p} , the achieved rate region \mathcal{R}_L^P is the same as \mathcal{R}_L^S [38]. Analytically,

$$\mathcal{R}_L^P = \left\{ \begin{array}{l} (r_1, r_2) : \\ 0 \leq r_1 \leq \alpha \Rightarrow 0 \leq r_2 \leq \frac{\alpha - (1 - \beta)r_1}{\alpha} \\ \alpha \leq r_1 \leq 1 \Rightarrow 0 \leq r_2 \leq \frac{\beta(1 - r_1)}{1 - \alpha} \end{array} \right\}. \tag{1.23}$$

¹ The normalization is done so that the links get unit rate when they transmit in isolation.

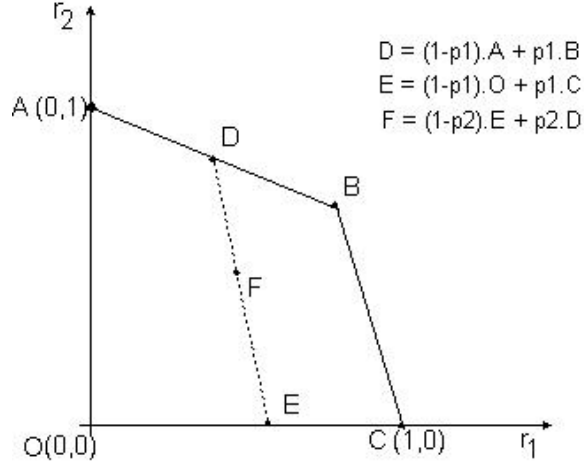


Fig. 1.3. \mathcal{R}_L^S and \mathcal{R}_L^P for the case $\alpha + \beta \geq 1$. $\mathcal{R}_L^P \equiv \mathcal{R}_L^S$ and is given by the area enclosed by $OABC$. B represents (α, β) .

High Interference Case : $\alpha + \beta < 1$

In this case, \mathcal{R}_L^S is given by the triangle formed by points O , A and C in Figure 1.4. As in the previous case, point F in Figure 1.4 corresponds to the rate vector \mathbf{r} achieved for a given $\mathbf{p} = [p_1 \ p_2]^T$. If $p_1 = 1$, the line segment DE coincides with BC . As p_1 varies from 1 to 0, DE moves from BC to an intermediate position HG to finally AO (for $p_1 = 0$) tracing out the region \mathcal{R}_L^P as the area enclosed by $OAHIC$. Note that the boundary $AHIC$ of the region is convex and contains two linear components AH and IC . The presence of linear component AH can be geometrically understood by observing that as DE moves from HG to AO , endpoint D always lies on the linear segment AH . In order to intuitively understand the presence of IC , it helps to notice that as p_1 varies from 1 to 0, J , the point of intersection of DE and BC initially moves from B towards C , goes up to a certain point I , and then moves back towards B . The analytical characterization of the above region is given by [38]

$$\mathcal{R}_L^P = \left\{ \begin{array}{l} (r_1, r_2) : \\ 0 \leq r_1 \leq \frac{\alpha^2}{1-\beta} \Rightarrow 0 \leq r_2 \leq \frac{\alpha - (1-\beta)r_1}{\alpha}, \\ \frac{\alpha^2}{1-\beta} < r_1 < 1 - \beta \Rightarrow 0 \leq r_2 \leq \frac{(\sqrt{(1-\beta)r_1 - 1})^2}{1-\alpha}, \\ 1 - \beta \leq r_1 \leq 1 \Rightarrow 0 \leq r_2 \leq \frac{\beta(1-r_1)}{1-\alpha}. \end{array} \right\}. \quad (1.24)$$

1.5.3 Distributed Algorithm

In this section, we present a distributed algorithm to compute the probability vector \mathbf{p} corresponding to a feasible point in the rate region \mathcal{R}_L^P . Each link

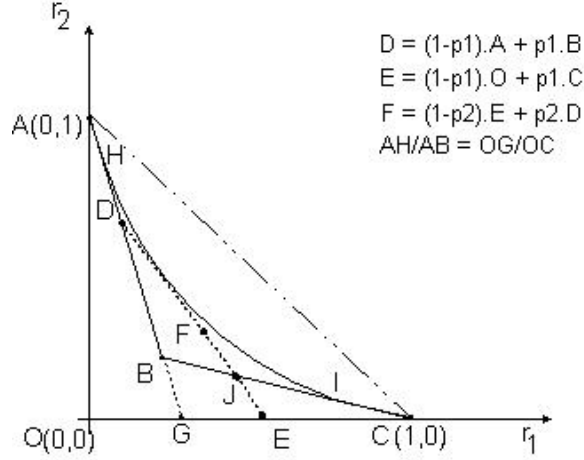


Fig. 1.4. \mathcal{R}_L^S and \mathcal{R}_L^P for the case: $\alpha + \beta < 1$. \mathcal{R}_L^S is given by the area enclosed by OAC and \mathcal{R}_L^P is given by the area enclosed by $OAHIC$. $B = (\alpha, \beta)$.

updates its probability of transmission based on the rate it achieves in the previous slot. We start by identifying a property of the function $r_i(\mathbf{p})$ that is the key for proving the convergence of our distributed algorithm.

The rate $r_i(\mathbf{p})$ achieved by link i in the random access scheme can be written as

$$r_i(\mathbf{p}) = \sum_{j=1}^M c_{ij} \prod_{l=1}^L [t_{lj}p_l + (1 - t_{lj})(1 - p_l)] \quad (1.25)$$

$$= p_i \sum_{j:t_{ij}=1} c_{ij} \prod_{l \neq i} [t_{lj}p_l + (1 - t_{lj})(1 - p_l)] \quad (1.26)$$

Let us define

$$g_i(\mathbf{p}_{-i}) = \sum_{j:t_{ij}=1} c_{ij} \prod_{l \neq i} [t_{lj}p_l + (1 - t_{lj})(1 - p_l)] \quad (1.27)$$

where

$$\mathbf{p}_{-i} = [p_1, \dots, p_{i-1}, p_{i+1}, \dots, p_L]^T \quad (1.28)$$

Then $r_i(\mathbf{p})$ can be written as

$$r_i(\mathbf{p}) = p_i g_i(\mathbf{p}_{-i}) \quad (1.29)$$

The following lemma states a property of $r_i(\mathbf{p})$, which is straight forward to prove [38].

Lemma 1. $g_i(\cdot)$ is a positive and strictly decreasing function of p_j for all $j \neq i$. Therefore, $r_i(\cdot)$ is a strictly increasing function of p_i and a strictly decreasing function of p_j for all $j \neq i$.

Now for each link i , consider the following iterative update of $p_i(n)$ based on the current rate $r_i(n)$ and the desired rate r_i^d . In practice the current rate $r_i(n)$ is measured by averaging the rates obtained over many slots.

$$p_i(n+1) = \frac{r_i^d}{r_i(n)} p_i(n) \quad (1.30)$$

Theorem 2. *Given a feasible rate vector $\mathbf{r}^d \in \mathcal{R}_L^P$, if all the links perform the above iteration independently starting with $\mathbf{p}(0) = \mathbf{0}$, then their iterations converge to a fixed point $(\mathbf{p}^*, \mathbf{r}^*)$ such that $\mathbf{r}^* = \mathbf{r}^d$ and $\mathbf{p}(n) \leq \mathbf{1}$ for all n .*

Proof. Using (1.29), we can rewrite (1.30) as

$$p_i(n+1) = \frac{r_i^d}{g_i(\mathbf{p}_{-i}(n))} \quad (1.31)$$

Substituting $\mathbf{p}(0) = \mathbf{0}$ in the iteration, we get $\mathbf{p}(1) = \mathbf{r}^d$ and therefore $\mathbf{p}(1) \geq \mathbf{p}(0)$. Using Lemma 1 with the above fact, it follows that $\mathbf{p}(2) \geq \mathbf{p}(1)$ and in general $\mathbf{p}(n+1) \geq \mathbf{p}(n)$ for all n . Therefore, if $\mathbf{p}(n)$ is bounded from above by $\mathbf{1}$, as n increases, it must converge to a fixed point \mathbf{p}^* and the corresponding \mathbf{r}^* is then equal to \mathbf{r}^d .

We now prove that if \mathbf{r}^d is feasible, then $\mathbf{p}(n)$ remains bounded below $\mathbf{1}$. Feasibility of \mathbf{r}^d means that there exists $\mathbf{0} \leq \mathbf{p}^d \leq \mathbf{1}$ such that

$$p_i^d = \frac{r_i^d}{g_i(\mathbf{p}_{-i}^d(n))} \quad (1.32)$$

By definition, $\mathbf{p}^d \geq \mathbf{p}(0)$. Using (1.31) and (1.32), we can see that $\mathbf{p}^d \geq \mathbf{p}(1)$ and in general $\mathbf{p}^d \geq \mathbf{p}(n)$ for all n . Therefore $\mathbf{p}(n)$ must also remain bounded below $\mathbf{1}$.

In case the users choose an infeasible \mathbf{r}^d , the above iteration will lead to a situation where some $p_i(n)$'s exceed 1. To avoid such infeasible conditions, we can modify the iteration to the one given below.

$$p_i(n+1) = \min \left\{ \frac{r_i^d}{r_i(n)} p_i(n), 1 \right\} \quad (1.33)$$

The above iteration converges to the desired rate vector \mathbf{r}^d if it is feasible.

1.6 Cross layer scheduling of end-to-end flows

Building up on the model described in Section 1.2, in this section, we discuss cross-layer scheduling of end-to-end flows in a cognitive wireless network with mutually interfering links. End-to-end rate guarantees through link scheduling have been well studied for wired networks [31]. However, rate guarantees in

wireless networks are difficult to handle because the shared wireless medium induces a large number of various scheduling constraints. The tutorial paper [25] summarizes some of the recent works on cross-layer optimization in wireless networks.

In [21], the author describes a model in which there exist multiple flows through finite capacity links. The problem is to find a set of optimal rates and flows that maximize a utility function of the source rates subject to constant link capacity constraints. However, our objective is to schedule the links for transmission and find optimal rates and flows subject to rate constraints in the links, due to interference from other links. In [36], the authors propose a fair scheduling algorithm that guarantees end-to-end max-min fair rates. The scheduling constraints are such that active links at any slot must constitute a matching. Our work provides a schedule which maximizes the sum of utility function of the source rates of origin-destination (OD) pairs, and fair scheduling can be brought out as a special case. The scheduling constraints can be very general and includes schedules consisting of matchings. In [24], the authors describe a cross-layer rate control and scheduling scheme. The rate in a link is a generic function (called the rate-power function) of transmission power of the link. The rates are lower bounded by the sum of source flows in the links. In this work, we provide an explicit characterization for the rate of a link. The rates are variable and depend logarithmically on the Signal-to-Interference Ratio (SIR) of the individual links.

Consider a wireless network with N nodes forming L links sharing a common spectrum. As described in Section 1.2, the network can be represented as a directed graph \mathcal{G} . Let us assume that the network consists of K sessions. A session is specified by an origin-destination (OD) pair. A route r is a sequence of links forming a path in the graph \mathcal{G} . We assume that there are R possible routes in the whole network. For a session k , the routes are specified by the $L \times R$ matrix \mathbf{A}_k with entries $\in \{0, 1\}$, where

$$[\mathbf{A}_k]_{lr} = \begin{cases} 1, & \text{if link } l \text{ is a part of route } r, \\ 0, & \text{otherwise.} \end{cases} \quad (1.34)$$

Let f_{kj} , $k = 1, \dots, K, j = 1, \dots, R$ be the flow corresponding to the k th session in the j th route. If \mathcal{R}_l denotes the set of routes passing through the link l , we can write the expression for the rate in link l in the session k as

$$r_{lk} = \sum_{j \in \mathcal{R}_l} f_{kj} = \mathbf{a}_{kl}^T \mathbf{f}_k, \quad (1.35)$$

where $\mathbf{f}_k = [f_{k1} \ f_{k2} \ \dots \ f_{kR}]^T$ is the vector of flows for the k th session, $k = 1, \dots, K$, and \mathbf{a}_{kl}^T is the l th row of \mathbf{A}_k . Let $\mathbf{r}_k = [r_{1k} \ r_{2k} \ \dots \ r_{Lk}]^T$, we can then write the link rate vector equation,

$$\mathbf{r}_k = \mathbf{A}_k \mathbf{f}_k. \quad (1.36)$$

Thus the aggregate rates through links $l = 1, 2, \dots, L$ are given by

$$\mathbf{r} = \sum_k \mathbf{A}_k \mathbf{f}_k. \quad (1.37)$$

Each OD pair k in our system gets a rate $y_k = \mathbf{1}^T \mathbf{f}_k, k = 1, \dots, K$. We are interested in maximizing $\sum_k U_k(y_k)$, the sum of utility functions of the rates in each session.

In a network of mutually L interfering links, all the $M = 2^L$ modes may not be valid for transmission. For instance, since the links share a common spectrum, the transmitter and receiver in a node operate in the same channel. Hence the node cannot transmit and receive simultaneously because of self-interference. We refer to this constraint as the *duplexing constraint*. The duplexing constraint implies that modes corresponding to the adjacent edges in the graph \mathcal{G} are invalid, i.e., the modes should constitute a matching.

We now specify the cross-layer optimization problem for maximizing the sum of utility functions of the rates in each session can be posed as the mathematical program:

$$\max \sum_k U_k(y_k) \quad (1.38)$$

$$\text{subject to } y_k = \mathbf{1}^T \mathbf{f}_k, \quad k = 1, \dots, K, \quad (1.38a)$$

$$\mathbf{r} = \mathbf{C}\mathbf{x}, \quad (1.38b)$$

$$\mathbf{r} \geq \sum_k \mathbf{A}_k \mathbf{f}_k, \quad (1.38c)$$

$$\mathbf{x} \in \mathcal{X}, \quad (1.38d)$$

$$\mathbf{f}_k \geq 0, \quad k = 1, \dots, K. \quad (1.38e)$$

The variables of the above optimization problem are $\mathbf{x}, \mathbf{f}_k, k = 1, \dots, K$. If the utility function $U_k(y_k) = y_k$, then (1.38) maximizes the sum of end-to-end flows of OD pairs. We then get a linear program which can be solved using standard techniques [2]. If $U_k(y_k) = \log(y_k)$, then (1.38) is a convex optimization problem, which solves for the proportional fair rates [21].

Note that (1.38b) and (1.38c) imply that the sum of the flows in each link is upper bounded by a quantity which depends on the schedule. However, in the model described in [21], each link has a finite capacity, which is a constant. The result of the optimization program (1.38) is a set of transmission modes along with the time fraction of operation of these modes and the flows in each route. Appropriate activity of the modes makes the transport of end-to-end flows possible.

1.7 Simulation Results

We discuss a simple illustrative example for flow-level scheduling in this section. We consider a network of five nodes in a line as shown in Figure 1.5,

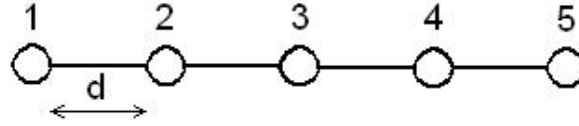


Fig. 1.5. Network with 5 nodes in a line. Each link is of length d

Table 1.1. Routes taken by the flow for different node separation distances

Range of d	Route (Sequence of links)	Transmission modes used
$0 \leq d \leq 4$	(1,5)	$\{(1,5)\}$
$4 < d \leq 6$	(1,3,5)	$\{(1,3)\}, \{(3,5)\}$
$6 < d \leq 8$	(1,3,4,5), (1,2,4,5)	$\{(1,2)\}, \{(1,3)\}, \{(2,4)\},$ $\{(3,4)\}, \{(1,2),(4,5)\}$
$d > 8$	(1,2,3,4,5)	$\{(1,2)\}, \{(2,3)\}, \{(3,4)\},$ $\{(1,2),(4,5)\}$

each node separated by a distance d from the other node. We label the nodes 1 through 5. These nodes form the vertices \mathcal{V} of a complete graph \mathcal{G} . Thus, there are ${}^5C_2 = 10$ links in the network. Each node may be able to transmit to any other in the network in just one hop. Because of the duplexing constraint, the links that transmit in any slot constitute a matching in the complete graph \mathcal{G} . Thus, the number of transmission modes in the network is equal to the number of non-trivial matchings in the \mathcal{G} , i.e., 25. The effect of interference between the links are captured by the matrix \mathbf{C} . The interference gain G_{lj} between the transmitter of link j and the receiver of a link l is given by $G_{lj} = d^{-4}$. The transmit powers are fixed for all transmissions.

We consider a single session originating at node 1 and ending at node 5. Note that there are 8 paths in the network for this OD pair. The objective is to maximize the flow in the network for the given OD pair. Given the distance d between the nodes, we can calculate the SIR for links in every possible mode and then construct the matrix \mathbf{C} for a fixed transmit power. By solving (1.38), we obtain the routes and the schedule for the modes required to obtain the optimal flows in these routes.

Figure 1.6 shows the variation of sum rate of flows with the distance d between any two nodes in the network. For small values of d , the direct hop is the most optimal route. This also results in the highest sum rate since the mode with the single link (1, 5) can be used. When d increases, there is a four fold increase in the length of direct hop link. Hence the flow between the OD pair decreases rapidly due to the path loss. As d increases further, the single hop link is no more optimal and the flow takes more than one hop to reach the destination. In our example, when $4 < d \leq 6$, two hops are required to maximize the flow. Since the nodes are equally spaced apart, the first hop is at the node 3. The flow decreases with increasing d , but for a two hop case, the link distance increases twice as d . For values of d in the range $6 < d \leq 8$,

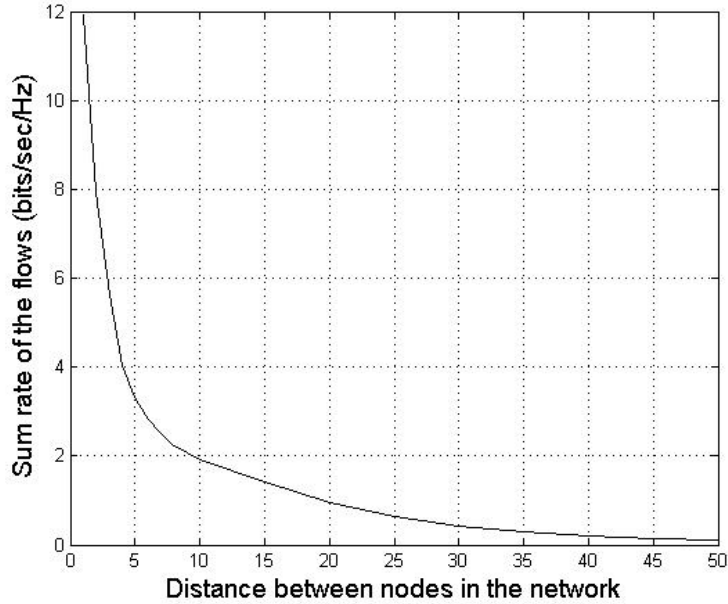


Fig. 1.6. Variation of source rates with the distance between the nodes for a fixed transmit power. $d = 10$ corresponds to 20 dB received SNR.

the flow is maximized when it takes three hops to the destination. For larger values of d , the flow is maximized when the each node transfers to the nearest neighbor and the flow takes 4 hops to the destination. The routes followed by the flows and the scheduled transmission modes are given in the Table 1.1.

1.8 Conclusion

Though link and flow level scheduling has received enough attention in literature, new emerging radio technologies offer additional degrees of freedom to the scheduling problem. In this chapter, we introduced the spectrum server that calculates efficient and fair time schedules. Performance of these schedules provide upper bounds for distributed scheduling schemes. We then study the loss in performance of a memoryless decentralized scheduling policy and provide a distributed algorithm that achieves any feasible rate vector. Finally, we extend the link scheduling framework to end-to-end flows in a network of mutually interfering links that support variable rates.

References

1. D. Bertsekas and R. Gallager. *Data Networks*. Prentice-Hall, 1992.
2. D. Bertsimas and J. Tsitsiklis. *Introduction to Linear Optimization*. Athena Scientific, 1997.
3. S. Boyd and L. Vandenberghe. *Convex Optimization*. Cambridge University Press, 2004.
4. M. Buddhikot, P. Kolodzy, S. Miller, K. Ryan, and J. Evans. DIMSUMNet: New directions in wireless networking using coordinated dynamic spectrum access. In *IEEE WoWMoM*, June 2005.
5. D. Cabric and R. W. Brodersen. Physical layer design issues unique to cognitive radio systems. In *Proc. IEEE PIMRC 2005*, 2005.
6. N. Clemens and C. Rose. Intelligent power allocation strategies in an unlicensed spectrum. In *Proc. IEEE DySPAN*, 2005. Baltimore, MD.
7. R. L. Cruz and A. V. Santhanam. Optimal link scheduling and power control in CDMA multihop wireless networks. In *IEEE Globecom*, pages 52–56, 2002.
8. R. L. Cruz and A. V. Santhanam. Optimal routing, link scheduling and power control in multi-hop wireless networks. *IEEE Infocom*, 2003.
9. T. Elbatt and A. Ephremides. Joint scheduling and power control for wireless ad-hoc networks. 3(1):74–85, Jan 2004.
10. A. Ephremides. Energy concerns in wireless networks. *IEEE Wireless Communications*, 9(4):48–59, Aug 2002.
11. R. Etkin, A. Parekh, and D. Tse. Spectrum sharing for unlicensed bands. In *Proc. IEEE DySPAN*, 2005. Baltimore, MD.
12. A. J. Goldsmith and S. B. Wicker. Design challenges for energy-constrained ad hoc wireless networks. *IEEE Wireless Communications*, 9(4):8–27, Aug 2002.
13. D. Goodman and N. Mandayam. Power control for wireless data. *IEEE Personal Communications*, 7:48–54, Apr 2000.
14. P. Gupta and A. Stolyar. Optimal throughput allocation in general random-access networks. In *Proc. CISS*, 2006. Princeton, NJ.
15. B. Hajek and G. Sasaki. Link scheduling in polynomial time. *IEEE Trans. Info. Theory*, 34(5):910–917, Sept 1988.
16. S. Haykin. Cognitive radio: brain-empowered wireless communications. *IEEE Journal on Selected Areas in Communications*, 23(2):201–220, Feb 2005.
17. J. Mitola III. *Cognitive radio: an integrated agent architecture for software defined radio*. PhD thesis, KTH Royal Institute of Technology, 2000.
18. O. Ileri, D. Samardzija, T. Sizer, and N. Mandayam. Demand responsive pricing and competitive spectrum allocation via a spectrum policy server. In *Proc. IEEE DySPAN*, Nov 2005. Baltimore, MD.
19. M. Johansson and L. Xiao. Cross-layer optimization of wireless networks using nonlinear column generation. *IEEE Trans. Wireless Commun.*, 5(2):435–445, Feb 2006.
20. K. Kar, S. Sarkar, and L. Tassiulas. Achieving proportional fairness using local information in ALOHA networks. *IEEE Trans. Auto. Control*, 49(10):1858–1862, Oct 2004.
21. F. Kelly. Charging and rate control for elastic traffic. *Euro. Trans. Telecommun.*, 8:33–37, Jan/Feb 1997.
22. L. Kleinrock and F. Tobagi. Packet switching in radio channels: Part i: Carrier sense multiple access and their throughput delay characteristics. *IEEE Trans. Communications*, 23(12):1400–1412, Dec 1975.

23. M. Kodialam and T. Nandagopal. Characterizing achievable rates in multi-hop wireless networks: the joint routing and scheduling problem. In *ACM Mobicom*, Sept 2003. San Diego, CA.
24. X. Lin and N. B. Shroff. The impact of imperfect scheduling on cross-layer rate control in multihop wireless networks. In *Proc. IEEE Infocom*, 2005.
25. X. Lin, N. B. Shroff, and R. Srikant. A tutorial on cross-layer optimization in wireless networks. *IEEE Journal on Selected Areas in Communications*, 24(8):1452–1463, Aug 2006.
26. J. Massey and P. Mathys. The collision channel without feedback. *IEEE Trans. Info. Theory*, 31(2):192–204, Mar 1985.
27. S. Mathur, L. Sankaranarayanan, and N. Mandayam. Coalitional games in receiver cooperation for spectrum sharing. In *Proc. CISS*, 2006. Princeton, NJ.
28. T. Nandagopal, T. -E. Kim, X. Gao, and V. Bhargavan. Achieving MAC layer fairness in wireless packet networks. In *Proc. ACM Mobicom*, pages 87–98, Aug 2000.
29. J. Neel and J. Reed. Performance of distributed dynamic frequency selection schemes for interference reducing networks. In *Proc. MILCOM*, 2006. Washington D.C.
30. N. Nie and C. Comaniciu. Adaptive channel allocation spectrum etiquette for cognitive radio networks. *ACM MONET (Mobile Networks and Applications), special issue on Reconfigurable Radio Technologies in support of ubiquitous seamless computing*, to appear 2006.
31. A. Parekh and R. Gallager. A generalized processor sharing approach to flow control - the single node case. *IEEE/ACM Trans. Networking*, 1(3):344–357, Jun 1993.
32. B. Radunovic and J. Y. L. Boudec. Rate performance objectives of multihop wireless networks. *IEEE Trans. Mobile Computing*, 3(4):334–349, Oct.-Dec 2004.
33. C. Raman, R. Yates, and N. Mandayam. Scheduling variable rate links via a spectrum server. In *Proc. IEEE DySPAN*, 2005. Baltimore, MD.
34. A. Sahai, N. Hoven, and R. Tandra. Some fundamental limits on cognitive radio. In *Proc. of Allerton Conf. on Comm., Control and Computing*, Oct 2004.
35. A. Sahai, R. Tandra, S. M. Mishra, and N. Hoven. Fundamental design trade-offs in cognitive radio systems. In *Proc. TAPAS*, Aug 2006.
36. S. Sarkar and L. Tassiulas. End-to-end bandwidth guarantees through fair local spectrum share in wireless ad hoc networks. *IEEE Trans. Auto. Control*, 50(9):1246–1259, Sept 2005.
37. S. Shakkottai and A. Stolyar. Scheduling for multiple flows sharing a time-varying channel: The exponential rule. *American Mathematical Society Translations*, 207, 2002.
38. J. Singh, C. Raman, R. Yates, and N. Mandayam. Random access for variable rate links. In *Proc. MILCOM 2006*, Oct 2006. Washington D.C.
39. V. Srivastava, J. Neel, A. MacKenzie, J. Hicks, L.A. DaSilva, J.H. Reed, and R. Gilles. Using game theory to analyze wireless ad hoc networks. *IEEE Communications surveys and tutorials*, 4th quarter 2005.
40. L. Tassiulas and A. Ephremides. Jointly optimal routing and scheduling in packet radio networks. *IEEE Trans. Info. Theory*, 38(1):165–168, Jan 1992.
41. L. Tassiulas and S. Sarkar. Maxmin fair scheduling in ad hoc wireless networks. *IEEE Journal on Selected Areas in Communications*, 23(1):163–173, Jan 2005.

42. P. Viswanath, D. Tse, and R. Laroia. Opportunistic beamforming using dumb antennas. *IEEE Trans. Info. Theory*, 48(6):1277–1294, Jun 2002.
43. H. Viswanathan and S. Mukherjee. Throughput-range tradeoff of wireless mesh backhaul networks. *IEEE Journal on Selected Areas in Communications*, 24(3):593–602, Mar 2006.
44. A. J. Viterbi. *CDMA: Principles of Spread Spectrum Communication*. Addison Wesley, 1995.
45. X. Wang and K. Kar. Distributed approaches for proportional and max-min fairness in random access ad hoc networks. In *Proc. CISS*, 2006. Princeton, NJ.
46. R. Yates, C. Raman, and N. Mandayam. Fair and efficient scheduling of variable rate links via a spectrum server. In *Proc. IEEE ICC*, Jun 2006. Istanbul, Turkey.
47. Q. Zhao, L. Tong, A. Swami, and Y. Chen. Decentralized cognitive MAC for opportunistic spectrum access in ad hoc networks: A POMDP framework. *IEEE Journal on Selected Areas in Communications*, to appear 2007.
48. H. Zheng and L. Cao. Device-centric spectrum management. In *Proc. IEEE DySPAN*, 2005. Baltimore, MD.

Index

bottleneck, 9

centralized scheduling, 1, 2
convex optimization, 10
cross-layer, 16

device-centric, 11
directed graph, 4
distributed algorithm, 14
dominant mode, 3
duplexing constraint, 18

matching, 19
max-min fair, 3, 8
mode activity vector, 4

pareto boundary, 11
proportional fair, 3, 10

rate region, 12

spectrum server, 1–3

transmission mode, 4

